

Supplementary information for:

Ferromagnetism in Semiconducting Janus NbSe Hydride Monolayer

Xiaocheng Zhou, Xu Sun, Zhuhua Zhang*, Wanlin Guo*

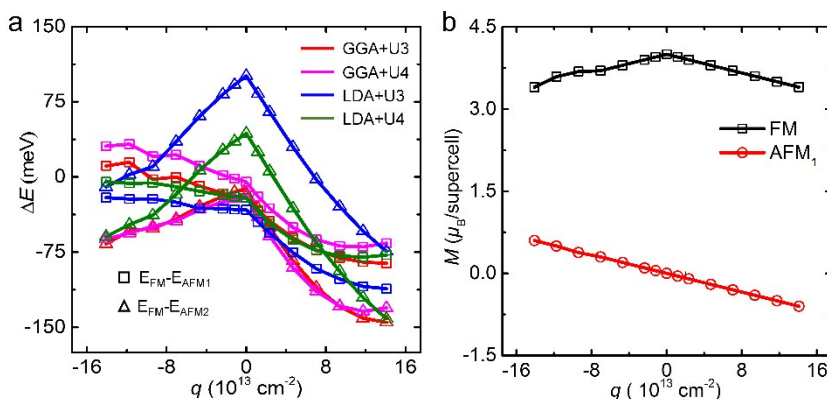


Fig. S1. Magnetic modulation of the NbSeH₂ monolayer. (a) Energy differences between the FM and AFM₁ states, and between the FM and AFM₂ states as functions of charge-doping levels. The red, magenta, blue and green lines correspond to the GGA+U ($U_{\text{eff}} = 3$ eV), GGA+U ($U_{\text{eff}} = 4$ eV), LDA+U ($U_{\text{eff}} = 3$ eV) and LDA+U ($U_{\text{eff}} = 4$ eV) methods, respectively. (b) Total magnetic moment of the supercell in FM and AFM₁ configurations as a function of charge-doping levels.

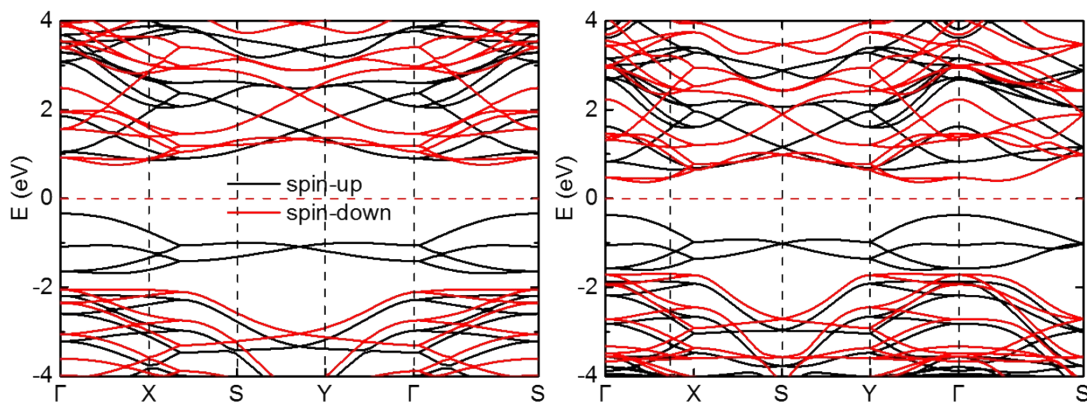


Fig. S2. Spin-resolved band structures calculated with (left) HSE06 and (right) LDA+U ($U_{\text{eff}} = 3$ eV) methods.

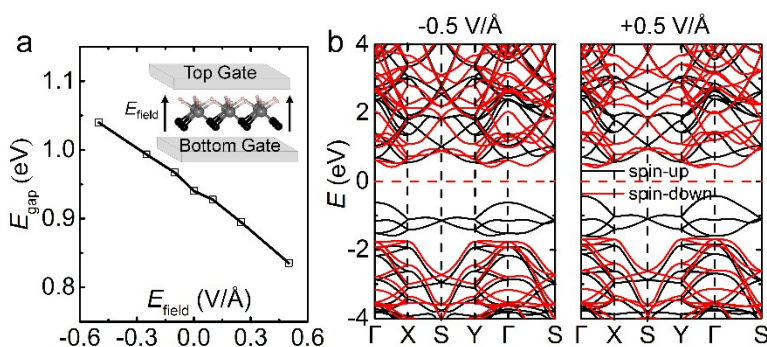


Fig. S3. Electronic modulation of the NbSeH₂ monolayer by vertical electric field. (a) Bandgap of the NbSeH₂ monolayer as a function of the strength of applied vertical electric field. Insert: A schematic diagram of the vertical electric field applied on the NbSeH₂ sheet. (b) Calculated spin-resolved band structures of NbSeH₂ under the vertical electric field of ± 0.5 V/Å.

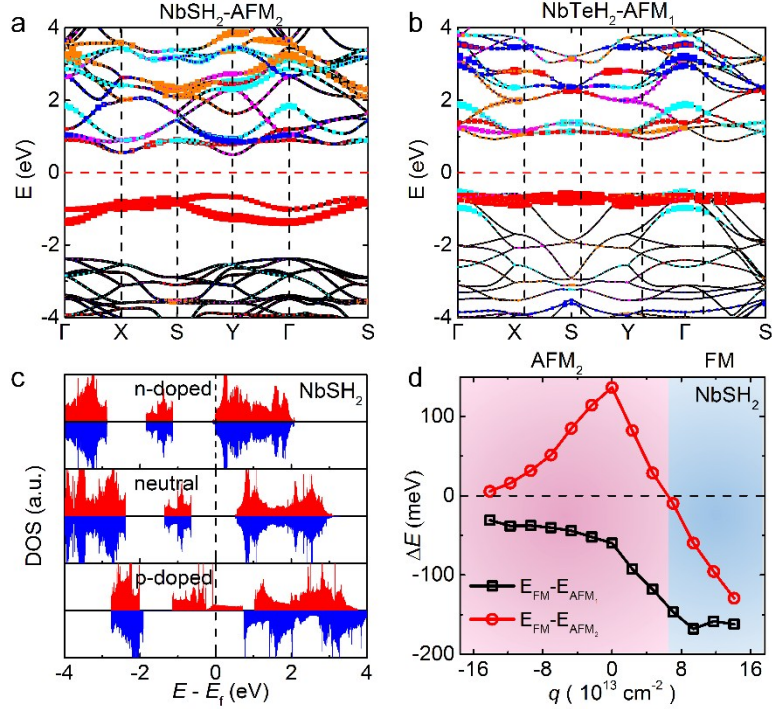


Fig. S4. Electronic properties of NbSH₂ and NbTeH₂ monolayers and magnetic modulation of the NbSH₂ monolayer. Spin-resolved band structures of (a) NbSH₂ in AFM₂ state and (b) NbTeH₂ in AFM₁ state. The orbital components of the bands are encoded by thickness and colors. (c) Spin-resolved density of states at the neutral state and at doping levels of $q = \pm 1.17 \times 10^{14} \text{ cm}^{-2}$ for NbSH₂ as an example. Red and blue areas represent the spin-up and spin-down states, respectively. (d) Energy differences of NbSH₂ between the FM and AFM₁ states, and between the FM and AFM₂ states as functions of charge-doping levels.

The calculated $E_{\text{FM}} - E_{\text{AFM}_2}$ is only -11.43 meV/supercell with GGA+U ($U_{\text{eff}} = 3$ eV) method, while $+8.79$ meV/supercell via HSE06 method. So the NbSeH₂ monolayer probably exhibits a paramagnetism state at room temperature. To gain more insight into the magnetic coupling, we computed the spin-polarized projected density of states (PDOS) for the Nb 4d orbitals in Fig. S5. The Se 3p states contribute little moment and thus are not discussed here. As shown in Fig. S5a, left panel, the wide peaks of ferromagnetic PDOS near the Fermi level indicate that the 4d orbitals are delocalized near the Fermi level, which favors ferromagnetism. While in Fig. S5a, right panel, the Nb 4d_{z²} orbitals show a localized state near the Fermi level, which may be favorable to antiferromagnetism. The magnetic ground state may be determined by the competition between ferromagnetic and antiferromagnetic exchange couplings. Furthermore, the delocalized PDOS at

the Fermi level under the hole-carrier doping (Fig. S5b, left panel) enhances the ferromagnetic coupling while the localized PDOS at the Fermi level under the electron-carrier doping (Fig. S5c, middle panel) turns the magnetic ground state into the nearest-neighbor antiferromagnetism.

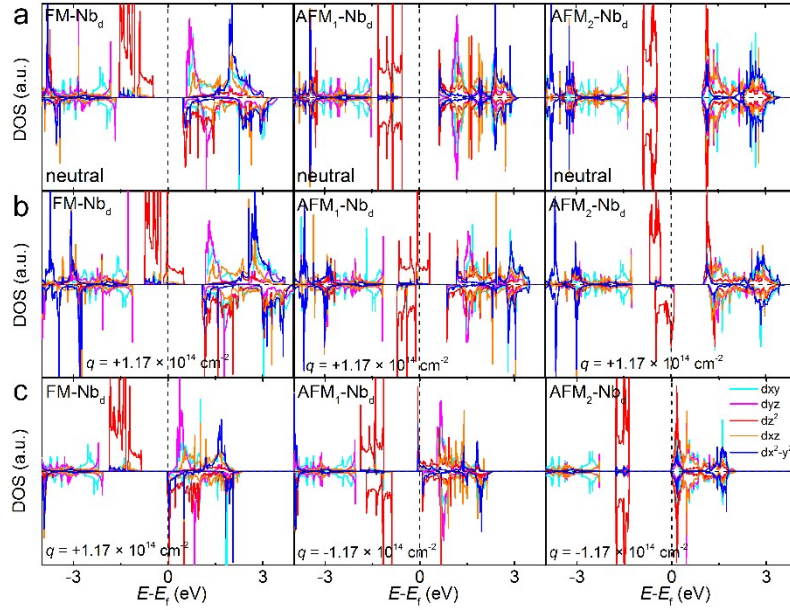


Fig. S5. Electronic properties of the NbSeH₂ monolayer. Spin-polarized PDOS for the Nb 4d orbitals (a) at the neutral state, at doping levels of (b) $q = +1.17 \times 10^{14} \text{ cm}^{-2}$ and (c) $q = -1.17 \times 10^{14} \text{ cm}^{-2}$. The d_{xy} , d_{yz} , d_z^2 , d_{xz} , $d_{x^2-y^2}$ orbitals of Nb atom are shown with multicolor lines.